IJSRA

International Journal of Science and Research Archive

eISSN: 2582-8185

Cross Ref DOI: 10.30574/ijsra

Journal homepage: https://ijsra.net/

(Research Article)

BASELINE PERFORMANCE ASSESSMENT OF A LOCALLY FABRICATED MICRO-JET ENGINE

Gbadebo Omoniyi Adeniyi [1,*], Aremo Emmanuel Akindele [2], Clement Idowu Ogunro [2], Remigious Adelakun Adamolekun [2], Samuel Okemute Egwenu [2] and Ganiyu Ayodele Odunaiya [2]

[1] Mission Operations and TT&C Division, Bola Ahmed Tinubu Centre for Space Transport and Propulsion, LASU Epe Campus, Lagos, Nigeria.
[2] Rocket System Engineering Division, Bola Ahmed Tinubu Centre for Space Transport and Propulsion, LASU Epe Campus, Lagos, Nigeria.
* Corresponding Author

ORCID Details
Gbadebo Omoniyi Adeniyi: https://orcid.org/0009-0001-1820-5966
Aremo Emmanuel Akindele: https://orcid.org/0009-0000-0190-6881
Clement Idowu Ogunro: https://orcid.org/0009-0003-4164-7177
Remigious Adelakun Adamolekun: https://orcid.org/0009-0008-2501-128X
Samuel Okemute Egwenu: https://orcid.org/0009-0002-9005-4100
Ganiyu Ayodele Odunaiya: https://orcid.org/0009-0000-4874-3784

International Journal of Science and Research Archive, 2026, 20(03), 055–066

Publication history: Received on 24 July 2026; revised on 31 August 2026; accepted on 02 September 2026

Article DOI: https://doi.org/10.30574/ijsra.2026.20.3.1702

ABSTRACT

In pursuit of indigenous technological capability in aerospace propulsion, this paper presents the design, development, and operational testing of a small-scale jet engine targeting a nominal thrust output of 250 N. The primary objective was to demonstrate the mechanical workability, aerodynamic integration, and structural integrity of locally fabricated components under operational run conditions. Experimental validation was conducted using a dedicated static test rig to evaluate ignition characteristics, rotational stability, and thermal performance during baseline runs. Test results confirmed the functional viability of the integrated turbomachinery assembly, establishing essential baseline datasets regarding mass flow efficiency, rotor dynamics, and thrust output. These empirical findings provide a benchmark for future iterative design improvements, particularly in turbine thermal tolerance and combustion efficiency.

Keywords: Aerospace propulsion, Indigenous technology, Micro-turbojet, Static thrust testing, Turbomachinery design.

1 INTRODUCTION

Jet engines remain indispensable to both military and commercial flight. Over a decade, the aviation and propulsion researches heavily focused on enhancing fuel economy, lowering emissions, integrating advanced materials, and adopting intelligent diagnostics. While high-bypass turbofans have historically led commercial aviation due to their quiet and efficient operation, the industry is pivoting toward next-generation set-ups. These include geared turbofans, hybrid-electric designs, and open-fan architectures. By removing the traditional protective nacelle, open-fan designs can boost propulsive efficiency and cut fuel consumption by up to 20%, though they also present fresh engineering hurdles regarding passenger safety and acoustic management [1]. Advanced materials like Ceramic Matrix Composites (CMCs) and nickel-based superalloys enhance jet engine efficiency by enabling higher turbine inlet temperatures, reducing cooling needs, and increasing extreme-condition durability. Additionally, 3D printing (additive manufacturing) cuts weight and improves combustion efficiency by enabling highly complex component designs [2]. Modern jet engine design prioritizes the aerodynamic optimization of compressor and turbine stages. High-pressure ratio compressors and refined blade aerodynamics successfully enhance thrust-to-weight ratios while reducing fuel consumption. Key emerging innovations driving these performance gains include variable cycle engines, composite fan blades, and optimized bypass ratios. For example, the CJ-1000A engine utilizes these advanced configurations to maximize overall efficiency and reliability [3].

Driven by environmental concerns, aviation research is rapidly pivoting toward cleaner propulsion technologies like Sustainable Aviation Fuel (SAF), hydrogen power, and hybrid-electric systems. Major programs like the CFM RISE initiative are spearheading this shift by utilizing innovative open-rotor configurations. These combined efforts aim to drastically reduce fuel burn and carbon emissions to support global sustainability goals [4]. Driven by increased computational power and the availability of massive datasets, data-driven approaches have become the leading methodology in jet engine research. Studies demonstrate that deep learning models substantially increase failure prediction accuracy and lower maintenance costs, while newer domain adaptation techniques successfully allow these models to generalize across highly variable engine operating conditions [5]. Prognostics and Health Management (PHM) systems have become indispensable for modern jet engines, employing advanced algorithms to simultaneously predict component failure modes and remaining useful life. By utilizing hybrid AI models that merge statistical methods with neural networks, these systems drastically reduce prediction errors while maintaining high computational efficiency [6]. Improving combustion efficiency is highlighted as key to maximizing engine performance. Later work further developed integrated thermodynamic analysis frameworks [7]. Turbofan engines dominate aviation because of their high efficiency, low noise, and high thrust. Recent studies show performance gains come from high bypass ratios, advanced compressors, and improved turbine cooling, though durability of high-temperature components remains a challenge [8]. Jet engine research now prioritizes sustainability through technologies like lean-burn combustors, increased bypass ratios, composites, and health monitoring systems. While their integration greatly reduces emissions and fuel use, cost and implementation barriers still persist [9][10].

Over the past decade, the integration of Artificial Intelligence and Machine Learning has revolutionized jet engine health monitoring. Key advancements include deep learning-based predictive maintenance, real-time sensor diagnostics, and digital twin technology for virtual lifecycle management. [14]. Exergy-based thermodynamic analysis is a key tool for assessing jet engine performance and component inefficiencies. In turbofan engines, the combustion chamber has the greatest exergy destruction, while turbines show comparatively less [17]. Recent research has shifted toward next-generation propulsion systems aimed at achieving net-zero emissions. Emerging technologies, including: Hydrogen-powered jet engines, Sustainable Aviation Fuels (SAF), Open-fan (open-rotor) architectures, Pressure-gain combustion systems [16]. These innovations aim to improve fuel efficiency while reducing carbon emissions and noise levels. Between 2020 and 2025, there has been rapid growth in the application of Artificial Intelligence (AI) in jet engine health monitoring. The use of Bi-Directional Long Short-Term Memory (BLSTM) models for predicting Remaining Useful Life (RUL) of turbofan engines using sensor data [15]. These approaches improve maintenance scheduling and reduce operational risks [13]. Similarly, explored domain adaptation techniques for improving prediction accuracy under varying operating conditions, highlighting the importance of data-driven prognostics in modern aviation systems [11]. Modern jet engine research increasingly depends on computational modeling, with surrogate modeling and active learning now used to accelerate design optimization. These methods deliver high accuracy at low computational cost, enabling faster iterations and better performance while cutting experimental expenses [12].

Jet engine technology has advanced rapidly due to efficiency, environmental, and digital drivers, leveraging thermodynamics, materials science, and AI. Future research is expected to prioritize indigenous efforts in developing sustainable jet engine systems and intelligent engine management solutions aligned with domestic capabilities.

2 MATERIAL AND METHODS

2.1 Jet Design and Fabrications

The jet components masses were calculated and appropriate materials selected for the design. Then, followed by the manufacturing through local procurement, dimension layout, cutting, folding, rolling, welding, finishing, and final test firing. The following are the designed jet components specifications. The intake (inlet) of a jet engine guides and slows incoming air smoothly into the compressor, while minimizing air-flow losses and turbulence. It also helps ensure a uniform, stable airflow to the engine (Table 1 and Figure 1a).

Table 1: Intake (Inlet) Specifications

Specifications	Values	Unit
Area of unit annulus geometry	0.069	m^2
Inlet Tip Diameter	0.316	m
Tip and Hub ratio	0.118	-
Mean diameter	0.214	m
Annulus blade heights	0.103	m

The compressor increases the pressure and temperature of the incoming air before it enters the combustion chamber, preparing it for efficient combustion (Table 2, Figure 1b).

Table 2: Compressor Specifications

Specifications	Values	Unit
Compressor outlet stagnation temperature	19.2	K
Compressor outlet temperature	333.6	K
Compressor outlet flow	0.028	kg/s
Outlet Annulus area	0.061	m^2
Outlet mean Diameter	0.272	m

The combustor (combustion chamber) mixes the compressed air with fuel and burns the mixture to produce high-temperature, high-energy gases that drive the turbine and generate thrust (Table 3 and Figure 1c).

Table 3: Axial Combustion Chamber Specifications

Specifications	Values	Unit
Stagnation temperature	352.55	K
Stagnation pressure	189187.35	N/m^2
Stagnation density	1.238	kg/m^3
Local acoustic velocity	371.35	m/s
Combustion chamber velocity	193	m/s
Mach number	0.520	-
Characteristics velocity	641.693	m/s
Combustion efficiency (%)	44.93	-
Throat area	0.052	m^2
Length of Combustion chamber	0.22	m
External volume of Combustion chamber	0.017	m^3
Volume of big inducer inside Combustion chamber	0.013	m^3
Area of big inducer inside Combustion chamber	0.026	m^2
Total internal area of Combustion chamber	0.349	m^2
Characteristic length of Combustion chamber	0.062	m

Thickness of Combustion chamber	0.0008	m
Exit Mach number	0.905	-

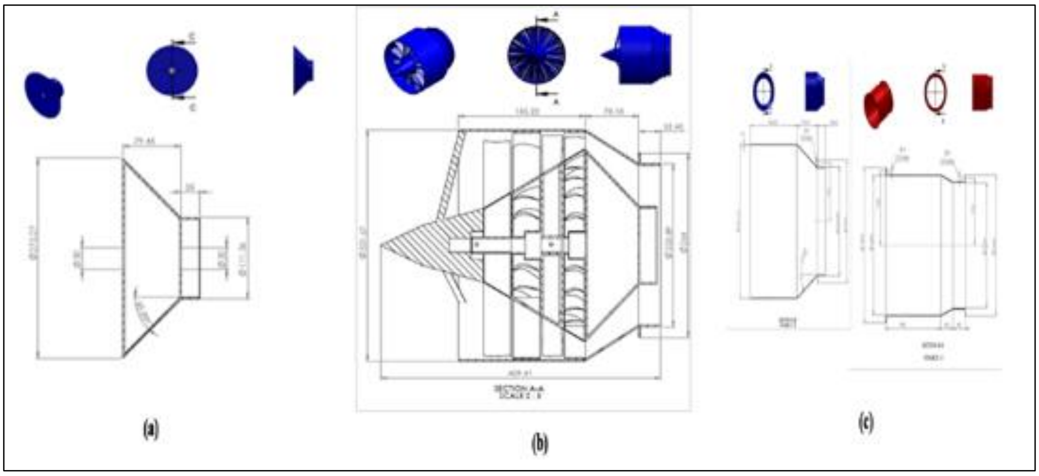

Figure 1: Jet component parts ((a) Inlet, (b) Compressor (c) Combustion Chamber)

The turbine extracts energy from the hot gases to drive the compressor and other engine accessories through a rotating shaft. It also helps the remaining gases produce thrust through the exhaust (Table 4 and Figure 2).

Table 4: Turbine Specifications

Specifications	**Values**	**Unit**
Area of Annulus geometry	0.059	m^2
Inlet Tip Diameter	0.279	m
Turbine rotational speed	32.887	rpm
Turbine overall efficiency (%)	56.01	-
Turbine outlet stagnation pressure	378374	N/m^2
Turbine outlet stagnation temperature	532.5	K
Outlet Tip Diameter	0.219	m

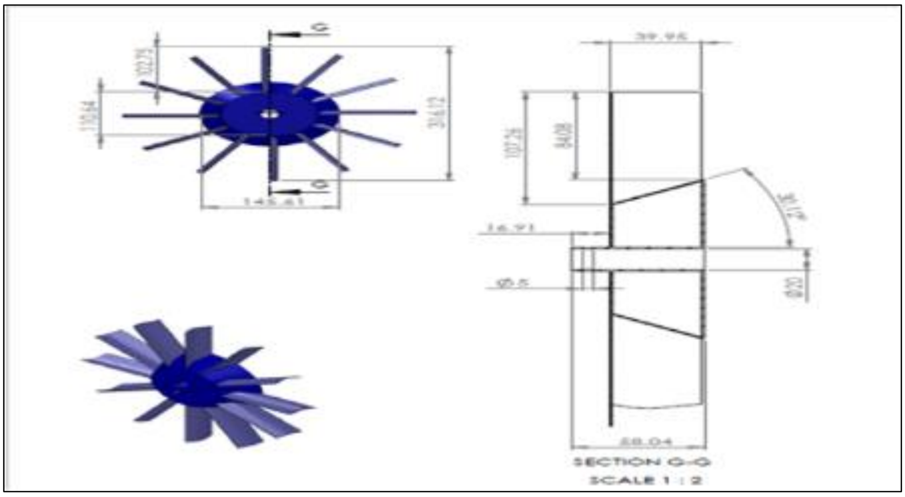

Figure 2: The Turbine Geometry

The exhaust nozzle accelerates the hot gases leaving the engine and converts their thermal energy into high-velocity exhaust, producing thrust to propel the aircraft forward (Table 5 and Figure 3).

Table 5: Exhaust Nozzle Specifications

Specifications	Values	Unit
Nozzle expansion	0.931	-
Exit area	0.029	m^2
Specific impulse	43.61	s
Force generated	6676.9	N
Thrust coefficient	0.680	-
Combustion chamber mass	0.038	kg

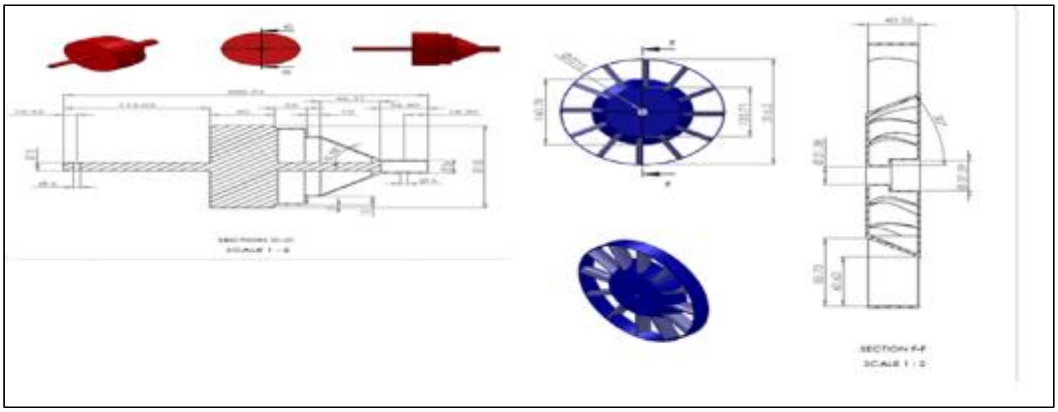

Figure 3: The Exhaust Nozzle

The stator is a stationary set of blades that guides and redirects the airflow between rotating stages, converting some velocity into pressure and improving the efficiency of the compressor or turbine (Table 6 and Figure 4).

Table 6: Compressor Specifications

Specifications	Values	Unit
Stage exit stagnation temperature	190	K
1st Stage outlet stagnation temperature	532.6	K
Stage pressure ratio	3.487	-
Stage outlet mass flow function	0.022	kg/s
Thickness of the Turbine	0.0028	m
Thrust of the Turbine	16094	N

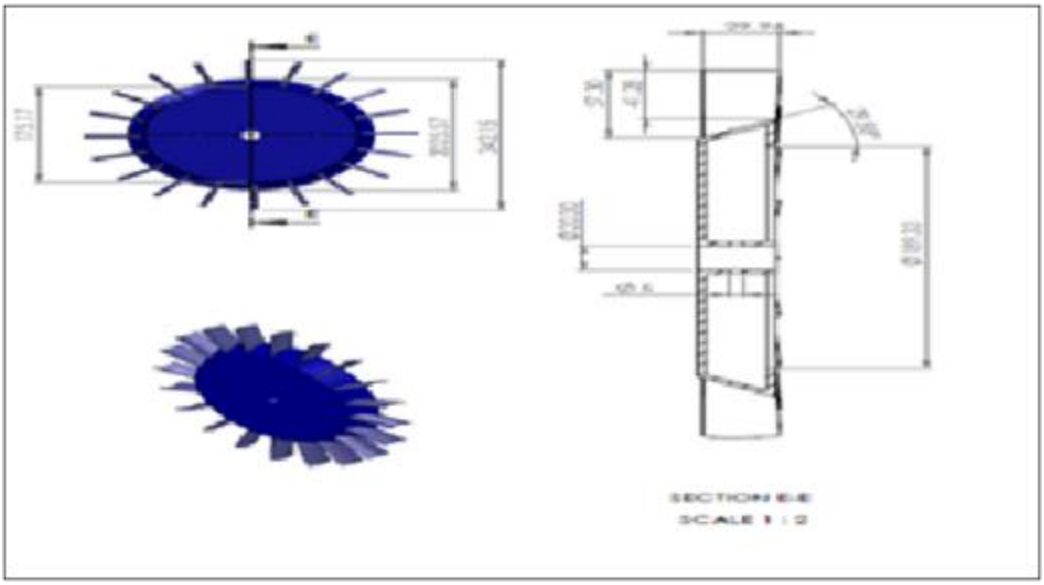

Figure 4: The Stator

The rotor is the rotating part of the engine that transfers energy between the airflow and the shaft, helping compress the air or extract energy from hot gases to drive the compressor (Table 7 and Figure 5).

Table 7: Rotor Compressor Inlet Annulus Geometry Specifications

Specifications	**Values**	**Unit**
Compressor outlet stagnation temperature	19.2	K
Compressor outlet temperature	333.6	K
Compressor outlet flow	0.028	kg/s
Outlet Annulus area	0.061	m^2
Outlet mean Diameter	0.272	m
Annulus blade height	0.045	m

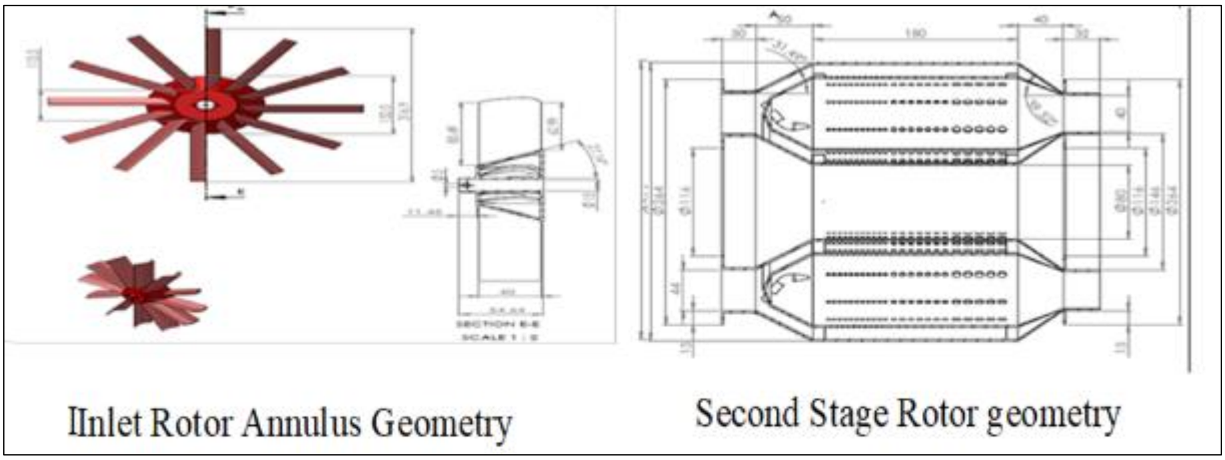

Figure 5: Inlet and Outlet Rotor Annulus Geometries

The inducer is the first part of a centrifugal compressor. It draws air into the compressor and accelerates it, preparing it for further compression (Table 8 and 9, Figure 6). The complete assembly of the compressor and the jet are shown in Figure 7 and Figure 8 respectively.

Table 8: Inducer Geometry Specifications

Specifications	Values	Unit
Volume of bigger inducer	0.013	m^3
Volume of smaller inducer	0.007	m^3
Total volume of inducer	0.006	m^3
Throat Diameter	0.257	m
Exit velocity of exhaust gas	26.49	m/s
Thickness of inducer	0.007	m
Bigger inducer area	0.026	m^2
Smaller inducer area	0.014	m^2

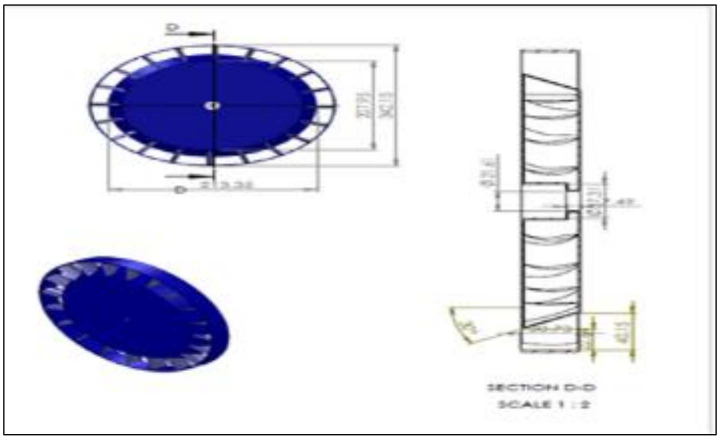

Figure 6: The Inducer

Table 9: Inducer Geometry Specifications

Specifications	Values	Unit
Stage exit stagnation temperature	9.6	K
1st stage outlet stagnation temperature	343.2	K
1st stage stagnation pressure	172304.6	N/m^2
Stage pressure ratio	1.089	-
Outlet Annulus area	0.058	m^2
Hub Diameter	0.166	m
Outlet mean Diameter	0.283	m
Outlet Annulus blade height	0.034	m

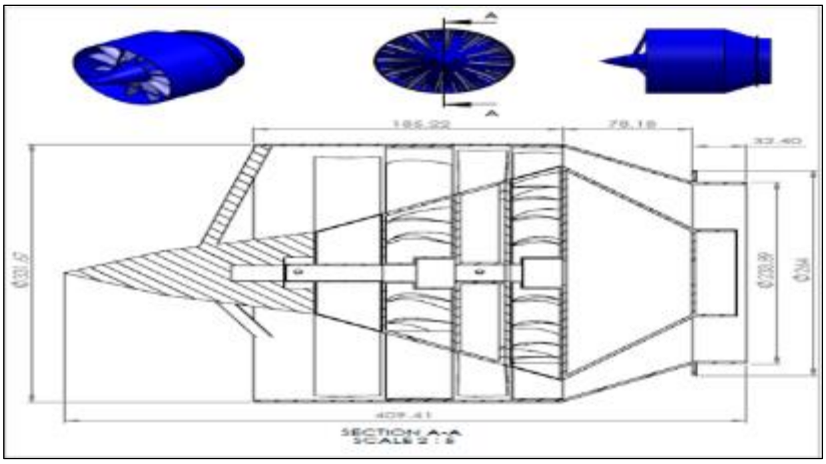

Figure 7: Complete Assembly of Compressor

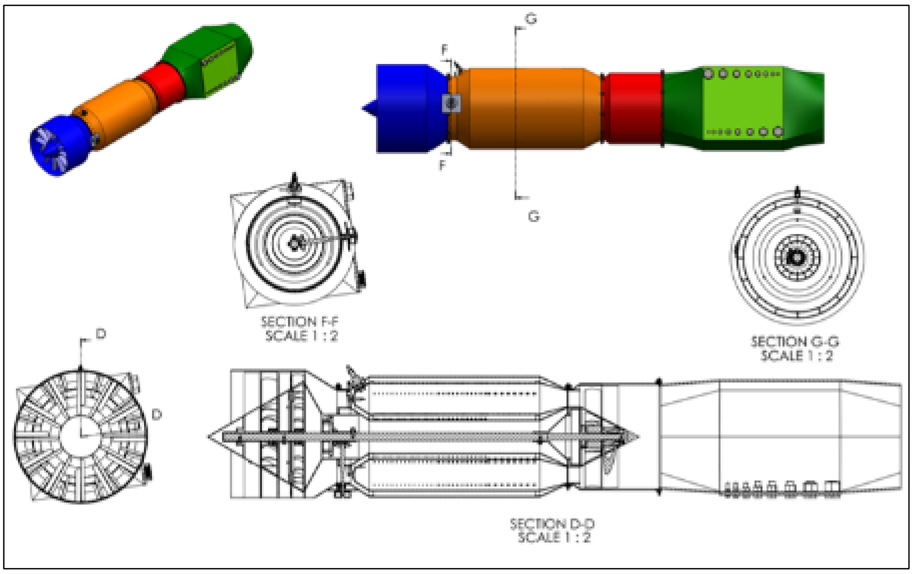

Figure 8: Complete Jet Assembly

2.2 Experimental Description

The designed jet engine features a single-spool configuration with a two-stage axial compressor comprising two rotor-stator pairs. A 12V DC starter motor mounted on the compressor casing drives the main shaft through a bevel gear system, directly coupling the compressor and turbine. Fuel is injected by three evenly spaced nozzles located around the exterior of the combustion chamber and directed into the inner liner. An igniter spark plug is positioned adjacent to the fuel nozzles to ensure reliable ignition. During startup, the starter motor spins the main shaft, driving the compressor and turbine to high speed, where compressed air mixes with kerosene and is ignited in the combustor. The resulting high-energy gases expand through the turbine and exhaust, and this process continues until the engine reaches self-sustaining operation.

2.3 Assembly and Ground Tests

The jet engine was validated on a static thrust stand with basic instrumentation to record thrust, fuel burn rate, shaft RPM, and exhaust gas temperature (EGT). Thrust was measured using a load cell, while shaft RPM was captured non-contact with an optical tachometer that counts light reflections from an LED beam on the rotating shaft. Fuel flow rate was determined by monitoring the mass loss of the fuel tank over time using a weighing scale. Prior to testing, the load cell was calibrated axially with known weights to generate a force curve. For startup, the fuel line was primed and the engine held at idle until temperatures stabilized. Baseline EGT and fuel consumption were then recorded. Finally, fuel mass flow rate and Thrust Specific Fuel Consumption (TSFC) were calculated at each operating point to evaluate overall efficiency, as shown in Equations 1 and 2.

Fuel Mass Flow Rate ($\dot{m}_f$):

$$\dot{m}_f = \frac{m_i - m_f}{\Delta t} \quad (1)$$

Thrust-Specific Fuel Consumption ($TSFC$):

$$TSFC = \frac{\dot{m}_f}{F} \quad (2)$$

3 RESULTS AND DISCUSSION

The results show a monotonic decrease in both fuel mass and mass flow rate with time. Conversely, both shaft velocity and propulsion efficiency exhibited a continuous increase over the test period. At t = 10 s, the system attained a maximum shaft velocity of 243.08 m/s and a propulsion efficiency of 100%, relative to the test conditions (Figure 9) and (Table 10).

Figure 9: Experimental installations and test

Table 10: Delivered Jet Performance Parameters

Operating Time (s)	Fuel masses (kg)	Fuel Mass Flow Rate (kg/s)	Shaft Velocity (m/s)	Propulsion Efficiency (%)	TSFC (for Thrust=250N) (kg/Ns)
0	8.0	0	0	0	0
2	7.74	0.13	37.87	33.3	0.00052
4	7.44	0.075	95.74	57.1	0.0003
6	7.18	0.043	125.61	75.0	0.00017
8	6.88	0.038	178.48	88.9	0.00015
10	6.62	0.026	243.08	100	0.00010

The performance trends observed in Table 10 provide insight into the transient behaviour of the propulsion system during fuel consumption. The mass of fuel decreased linearly from 8.00 kg to 6.62 kg over 10 s, resulting in a total fuel consumption of 1.38 kg. The mass flow rate, decreased from 0.130 kg/s at 2 s to 0.026 kg/s at 10 s. This reduction indicates that the fuel delivery rate was not constant but tapered with time. Such behaviour is typical of pressure-fed or blow-down propulsion systems where chamber pressure, and hence mass flow, decreases as propellant is depleted. The initial high mass flow rate at 2 s corresponds to the system start-up transient where maximum pressure is available.

The air velocity, increased progressively from 0 m/s to 243.08 m/s. This increase can be attributed to the inverse relationship between mass flow rate and exhaust velocity for a given thrust, as described by the momentum equation. As fuel mass flow rate decreased, the system appears to have converted the available energy into higher kinetic energy per unit mass of exhaust, leading to jet acceleration. The nearly six-fold increase in shaft velocity between 2 s and 10 s suggests improved energy conversion efficiency as the system stabilized.

Propulsion efficiency, increased from 33.3% to 100% over the same interval as indicated in Figure 10 and Figure 11. Propulsion efficiency for a jet in a simplified static test where vehicle velocity is zero, it is often normalized to the maximum attained value. The 100% value at 10 s therefore represents the peak efficiency achieved under the tested conditions, not necessarily the absolute thermodynamic efficiency. The increasing trend of propulsion efficiency correlates directly with the increase in shaft velocity and decrease in fuel mass flow rate. Higher shaft velocity relative to the mass flow implies that more useful propulsive work is being extracted per unit of fuel consumed. The low efficiency at 2 s is likely due to incomplete combustion, nozzle under-expansion, and system losses during ignition.

The inverse relationship between mass flow rate and both shaft velocity and efficiency is consistent with fundamental propulsion theory. As the system operates, reduced mass flow allows for more complete energy release and better expansion, resulting in higher specific impulse. The total fuel used of 1.38 kg over 10 s yielded a final shaft velocity of 243.08 m/s. This performance profile suggests that the system is more efficient at lower throttle settings later in the burn. For practical applications, this implies that optimizing the burn profile to operate at lower mass flow rates could maximize propulsion efficiency, albeit at the cost of thrust.

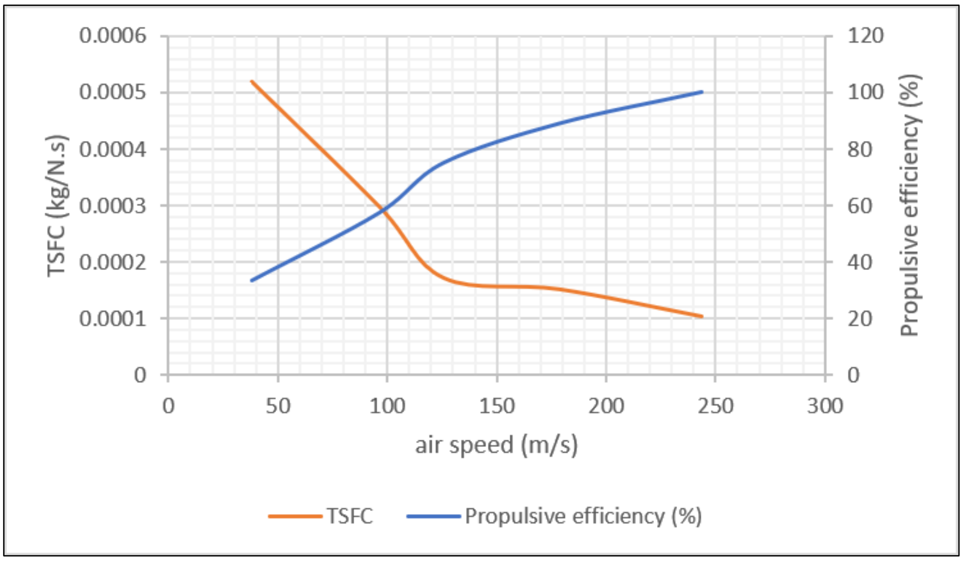

Figure 10: TSFC, Propulsive Efficiency against Air Speed

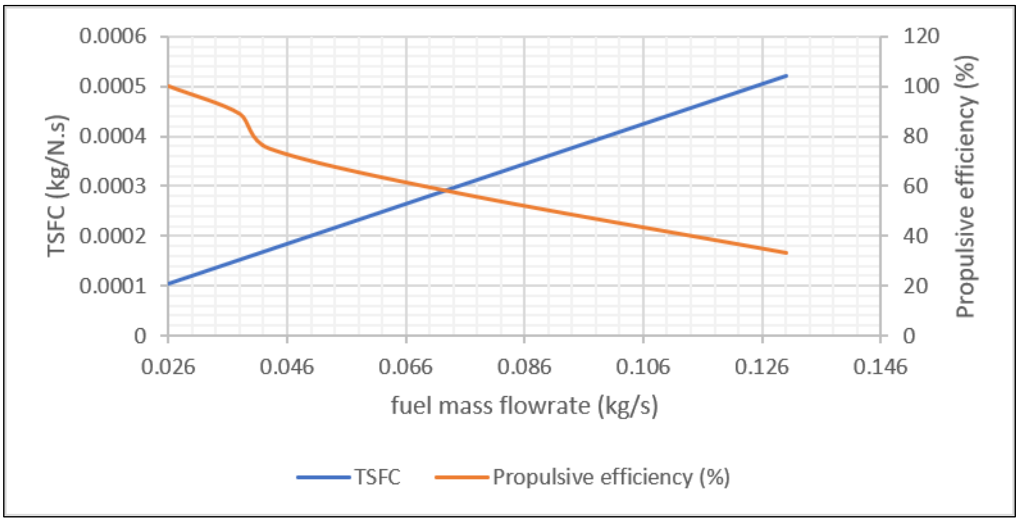

Figure 11: TSFC, Propulsive Efficiency Against Fuel Mass Flow Rate

4 CONCLUSION

This study successfully demonstrated the viability of an indigenously developed 250N class micro-turbojet engine, fulfilling the primary objective of validating the functional integration and mechanical workability of its core components. The measured critical baseline empirical data was gathered under the operational conditions. The successful operation of the prototype confirms that the baseline design architecture is sound, providing a verified experimental platform for subsequent technical iterations. To advance this technology toward operational deployment, future research should focus on optimizing combustion efficiency, improving turbine thermal resistance, and refining component aerodynamics to enhance power-to-weight performance.

STATEMENTS ON COMPLIANCE WITH ETHICAL STANDARDS

Acknowledgments

We acknowledged the efforts and contributions and supports of staff members of Bola Ahmed Tinubu Centre for Space Transport and Propulsion (BAT-CSTP), Epe, Lagos, Nigeria.

Funding Source

The project was funded by Bola Ahmed Tinubu Centre for Space Transport and Propulsion (BAT-CSTP), Epe, Lagos, Nigeria.

Disclosure of conflict of interest

There are no conflicts of interest.

REFERENCES

[1] Wang, Y., Ragab, M., Hou,Y., Wu, M., Li, X., and Chen, Z (2026). Deep Domain Adaptation for Turbofan Engine Remaining Useful Life Prediction: Methodologies, Evaluation, and Future Trends. IEEE/CAA J. Autom. Sinica. doi: 10.1109/JAS.2025.125843.

[2] Sherifi, A. (2024). Turbofan Engine Remaining Useful Life (RUL) Prediction Based on Bi-Directional Long Short-Term Memory (BLSTM)(arXiv). Computer Science-Machine Learning. https://doi.org/10.48550/arXiv.2411.16422.

[3] Cohen, J., Huan, X., & Ni, J. (2023). Fault prognosis of turbofan engines: Eventual failure prediction and remaining useful life estimation. International Journal of Prognostics and Health Management, 14(2), Article 3486. https://doi.org/10.36001/ijphm.2023.v14i2.3486

[4] Norris, G. (2021). CFM Unveils Open Fan Demonstrator Plan for Next-Gen Engine. Aviation Week & Space Technology, Vol. 183, pp. 34–39.

[5] Fehrm, B. (2023). Next Generation Aircraft Engine Architectures. Leeham News and Analysis, https://leehamnews.com/ Vol. 12, pp. 15–22.

[6] Ostrower, J. (2025). Advancements in High-Bypass Turbofan Engines. Aviation Week Network, Vol. 187, pp. 22–30.

[7] Patel, M. (2026). Future of Commercial Aircraft Engines and Certification Trends. OAG Aviation Report, Vol. 9, pp. 10–18.

[8] European Defence Industry Report (2025). Next Generation Fighter Engine Developments. EDR Magazine, Vol. 45, pp. 50–65.

[9] CFM International. (2023). RISE engine program overview (Technical Report). GE Aerospace & Safran Aircraft Engines. https://www.cfmaeroengines.com/rise

[10] Rolls-Royce (2022). UltraFan Engine Technology Demonstrator Report. Rolls-Royce Plc, Vol. 5, pp. 1–20.

[11] Şöhret, Y., Ekici, S., Altuntaş, Ö., Hepbasli, A., & Karakoç, T. H. (2016). Exergy as a useful tool for the performance assessment of aircraft gas turbine engines: A key review. Progress in Aerospace Sciences, 83, 57–69. https://doi.org/10.1016/j.paerosci.2016.03.001

[12] Aydin, H., et al. (2022). Energy, exergy, economic and environmental (7E) Analysis of turbofan engines. Energy Journal, Vol. 245, pp. 123–135.

[13] Sin, L. N. (2025). Research related to turbofan engines. Theoretical and Natural Science, 79(1), 33–37. https://doi.org/10.54254/2753-8818/2025.19935

[14] Pawar, A., and Dondapati, R. S. (2026). Multiphysics challenges in gas turbine blade design. International Journal of Turbo & Jet-Engines, Vol. 43(2), pp. 391–403.

[15] Ranasinghe, K., Guan, K., Gardi, A., & Sabatini, R. (2019). Review of advanced low-emission technologies for sustainable aviation. Energy, 188, Article 115945, 1–26. https://doi.org/10.1016/j.energy.2019.115945

[16] Xie, W. (2025). The Current Status and Future Development of Jet Engines. Vol. 160, pp. 565–572.

[17] Sherifi, A. (2024). Turbofan Engine Remaining Useful Life (RUL) Prediction Based on Bi-Directional Long Short-Term Memory (BLSTM). arXiv. https://doi.org/10.48550/arXiv.2411.16422

[18] Wang, Y., Ragab, M. Hou,Y., Chen, Z., Wu, M., Li, X. (2026). Deep domain adaptation for turbofan engine remaining useful life prediction: Methodologies, evaluation, and future trends. IEEE/CAA J. Autom. Sinica, Vol. 13, No. 8, pp. 1783–1803, doi: 10.1109/JAS.2025.125843.

[19] Abdelrehim, A., Gandhi, D., Yalburgi, S., Bharambe, A., Anantharaman, R., & Rackauckas, C. V. (2025). Active Learning Enhanced Surrogate Modeling of Jet Engines in JuliaSim. AIAA SCITECH 2025 Forum. https://doi.org/10.2514/6.2025-2323.